



Contents lists available at ScienceDirect

Journal of the Taiwan Institute of Chemical Engineers

journal homepage: www.elsevier.com/locate/jtice

Effective thermal conductivity of carbon nanotube-based nanofluid

Haifeng Jiang^a, Qiang Zhang^b, Lin Shi^{a,*}^a Key Laboratory for Thermal Science and Power Engineering of Ministry of Education, Department of Thermal Engineering, Tsinghua University, Beijing 100084, China^b Beijing Key Laboratory of Green Chemical Reaction Engineering and Technology, Department of Chemical Engineering, Tsinghua University, Beijing 100084, China

ARTICLE INFO

Article history:

Received 11 December 2014

Revised 23 March 2015

Accepted 29 March 2015

Available online xxx

Keywords:

Carbon nanotube

Nanofluid

Thermal conductivity

Aggregation

Nanostructured materials

ABSTRACT

The effective thermal conductivity of CNT/water nanofluid is measured with different CNT loadings (0.22–1 vol%) and temperatures (30–90 °C). The enhanced thermal conductivity increased nonlinearly with CNT concentrations while the ratios are almost constant with the rise of temperature. An aggregate-based model is proposed to predict the enhanced thermal conductivity of CNT-based nanofluid. The present model gives the lower and upper limits of CNT-based nanofluid with majority of the previous data fall within these bounds. CNT contact results in low-resistance heat conduction path which serves high thermal conductivity of nanofluid. The proposed model exhibits quite well an agreement with the experimental data and affords improved predictions for the enhanced thermal conductivity. The present study sheds light on the thermal conductivity mechanisms in CNT-based nanofluids with respect to CNT aggregate state in base fluids.

© 2015 Taiwan Institute of Chemical Engineers. Published by Elsevier B.V. All rights reserved.

1. Introduction

Nanofluids are suspensions of nanoparticles dispersed in conventional heat transfer fluids such as deionized water (DW), ethylene glycol (EG), and engine oil (EO) [1–3]. The nanofluids were found to exhibit more stable and higher thermal conductivity than those mixtures containing millimeter or micrometer-sized particles during the past decades [4–7]. When dispersed nanoparticle volume fractions were very low ($\varphi_p < 5$ vol%), the nanofluid exhibited striking high thermal conductivity which had been regarded as high efficient heat exchange fluid.

Carbon nanotubes (CNTs) have drawn worldwide attention since its discovery in 1991 [8]. CNTs are excellent nanoparticles for preparing nanofluids because they have superior thermal conductivity (750–6600 W/m K) [9–11] besides their high aspect ratio. The effective thermal conductivity of CNT-based nanofluids has been explored [12–20]. Choi et al. [12] reported a thermal conductivity enhancement of 156% for 1 vol% CNTs dispersed in synthetic poly- α -olefin oil (PAO). For DW, EG, and decene (DE)-based nanofluids with a CNT volume fraction of 1 vol%, Xie et al. [13] reported that the effective thermal conductivities were enhanced by 7%, 12.7%, and 19.6%, respectively. Recently, Liu et al. [18] measured the thermal conductivities of 1 vol% CNT-based nanofluids with the CNT outer diameter 20–50 nm and

about 9% and 12.4% enhancements were observed with EO and EG as the base fluids. Fig. 1 summarized the experimental data of thermal conductivity enhancement of CNT-based nanofluids. The relation between thermal conductivity enhancement (k_{nt}/k_{bf}) and CNT volume fraction (φ_p) was nonlinear, which was quite different from the linear relationship for nanofluids with spherical particles [2–7].

Various potential mechanisms that contribute to enhanced nanofluid thermal conductivity including nanoparticle Brownian motion, particle aggregation, nanolayer, ballistic transport and nonlocal effects, near-field radiation, and nanoparticle thermophoresis have been proposed [21–28]. Since their aspect ratio is high, CNTs easily aggregate or contact with each other in the base liquid. Aggregation model is one of the important mechanisms to explain the substantially high thermal conductivity of nanofluid [21,24–26]. Thermal conductivity enhancement contributions of other potential mechanisms such as Brownian motion and interfacial nanolayer were negligible [29]. Many researchers have proposed various models to explain the anomalous thermal conductivity of CNT-based nanofluids. However, the observed results of the effective thermal conductivity cover a wide range and the nonlinear relation between thermal conductivity enhancement and the CNT volume fraction cannot be satisfactorily predicted by these models [26,30].

In this study, the CNT/DW nanofluid stability was evaluated and the enhanced thermal conductivity as a function of CNT concentration and temperature between 30 and 90 °C was determined. A model based on the CNT aggregation was proposed and the present model compared well with majority of the available data considering the various concentrations of CNTs in the aggregates.

* Corresponding author. Tel.: +86 10 6278 7613; fax: +86 10 6278 7613.

E-mail address: rnxsl@mail.tsinghua.edu.cn, jhf1@mails.tsinghua.edu.cn (L. Shi).

Nomenclature

k_{nf}	nanofluid thermal conductivity (W/m K)
k_{bf}	base fluid thermal conductivity (W/m K)
k_p	nanoparticle thermal conductivity (W/m K)
k_{int}	aggregate thermal conductivity (W/m K)
k_{11}^c	CNT transverse equivalent thermal conductivity (W/m K)
k_{33}^c	CNT longitudinal equivalent thermal conductivity (W/m K)
φ_p	volume fraction of CNTs in base fluid
φ_a	volume fraction of aggregates in base fluid
φ_{int}	volume fraction of CNTs in aggregate
a_k	Kapitza radius (m)
R_k	interface thermal resistance ($m^2 K/W$)
d_p	CNT diameter (m)
L_p	CNT length (m)
β_{11} and β_{33}	dimensionless parameters

Subscripts

nf	nanofluid
bf	base fluid
p	nanoparticles in base fluid
int	nanoparticles in aggregate
a	aggregates in base fluid

2. Experimental procedure

The multi-walled CNTs (density 1.7 g/cm^3 , purity $> 97\%$) were produced by fluidized-bed chemical vapor deposition (FBCVD) method [31,32]. The base fluid DW (density 0.997 g/cm^3) was purchased from Tsinghua–Foxconn Nanotechnology Research Center, Beijing, China. The CNT/DW nanofluid was prepared by two-step method. The facile sheared CNTs were dispersed in DW using polyvinyl pyrrolidone (Aladin Industrial Corporation, Shanghai, China) as dispersant with the aid of magnetic force agitation (RET, IKA, Germany) for 30 min. The resultant suspension was then vibrated continuously by intensive

ultrasonication (JY98-IIIN, SCIENTZ, China) for 1 h to obtain a uniform nanofluid.

The transient hot-wire method was employed to measure the nanofluid thermal conductivity at temperature between 30 and 90°C . This technique was recognized as the most accurate method due to numerous advantages such as elimination of convection related to steady-state method and faster measurement response [33]. The schematic diagram and the measurement procedure had been explained previously in detail [6,7,34]. The apparatus was calibrated by measuring thermal conductivity of saturated liquid toluene (purity $> 99.5\%$) from 30 to 300°C and the maximum uncertainty was 0.55% [6,7].

3. Model formulation

Nan et al. [23] proposed a model including the effect of the interfacial resistance. The enhanced thermal conductivity of CNT-based

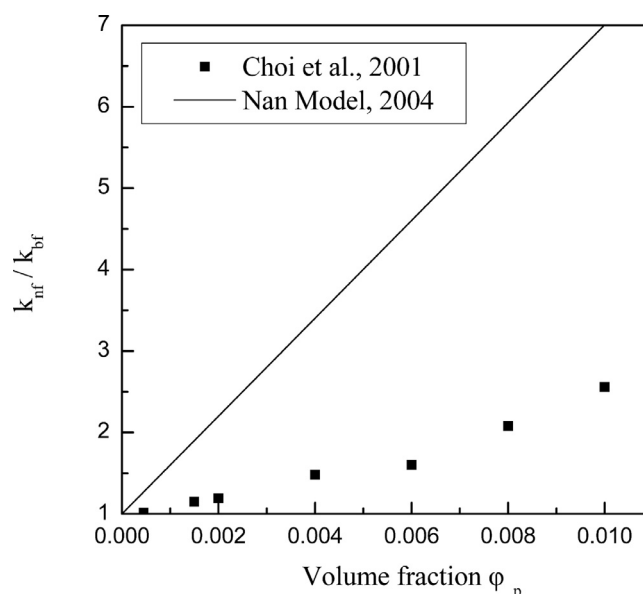


Fig. 2. Comparison of Nan model and experimental data [12].

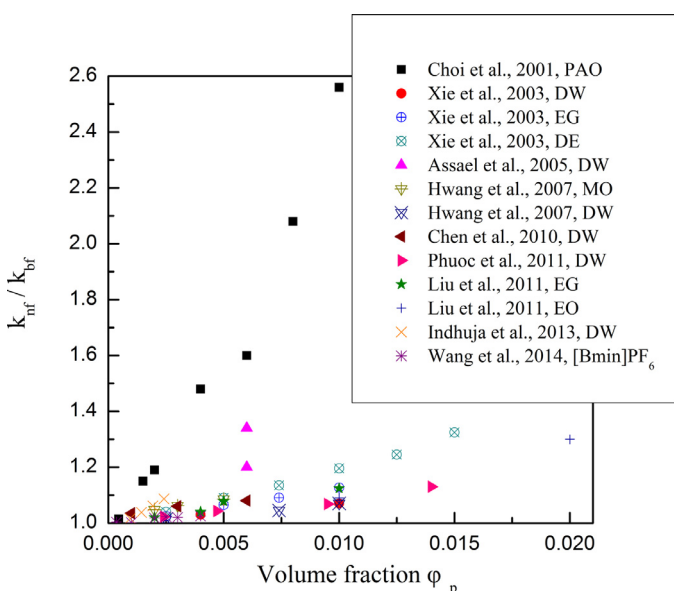


Fig. 1. Measured thermal conductivity of CNT-based nanofluids (base fluids: PAO means poly- α -olefin oil, DW means deionized water, EG means ethylene glycol, DE means decene, MO means mineral oil, EO means engine oil, and [B_{min}]PF₆ means 1-butyl-3-methylimidazolium hexafluorophosphate) [12–20].

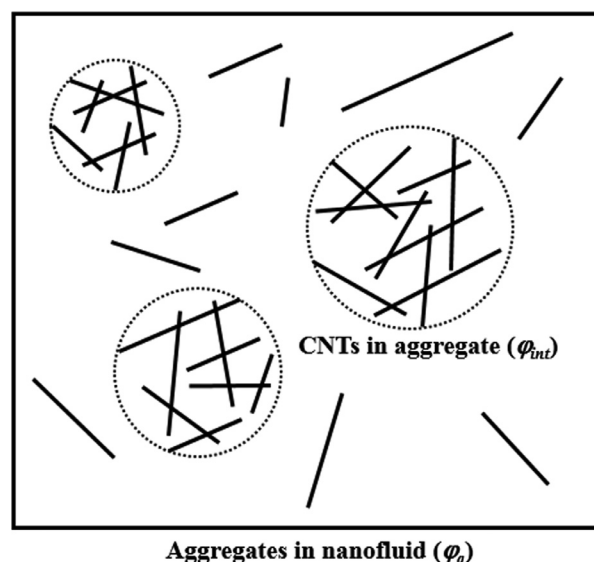


Fig. 3. Schematic of CNTs in aggregate (φ_{int}) and aggregates in nanofluid (φ_a).

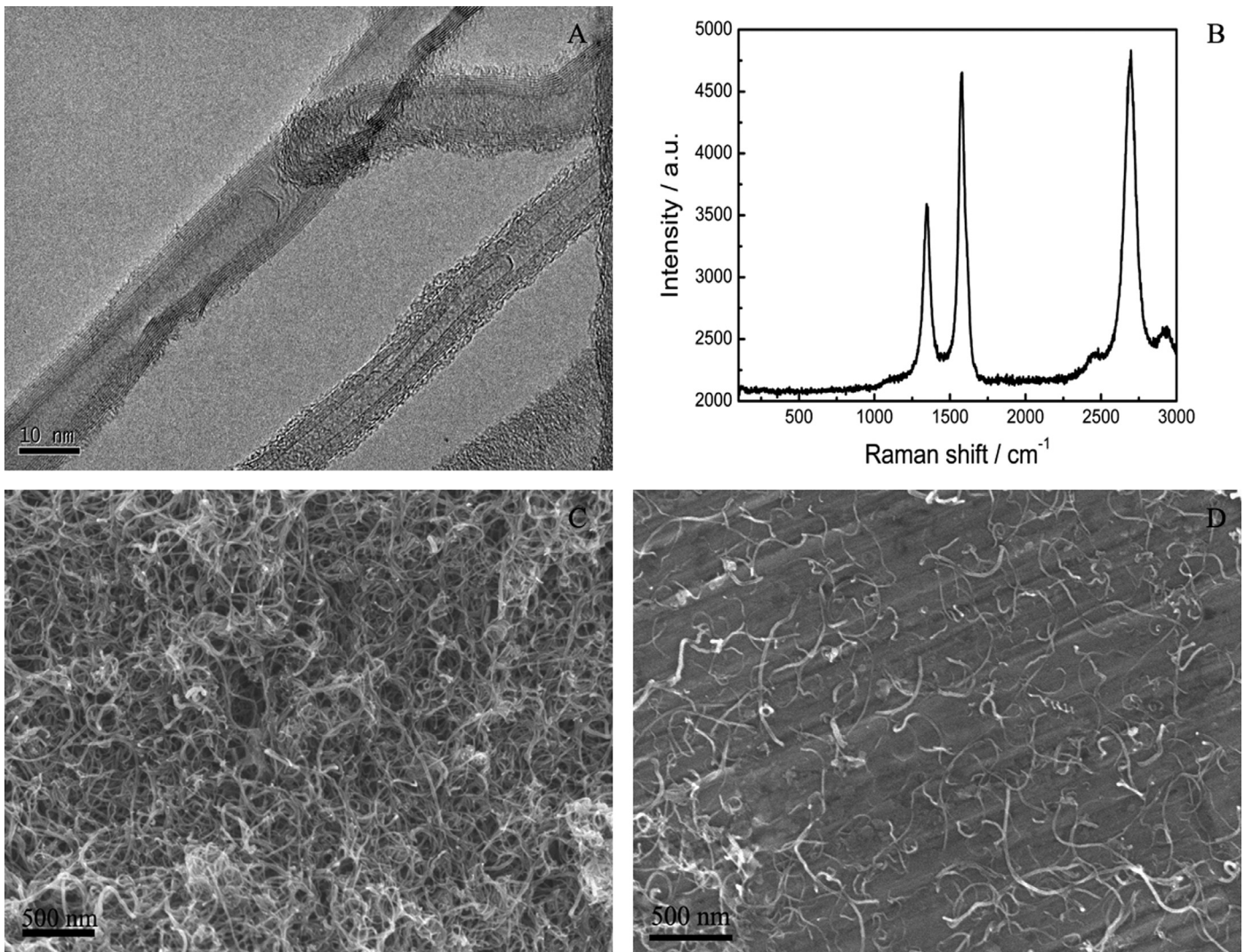


Fig. 4. Morphology of CNTs: (A) TEM photograph of pristine CNTs; (B) Raman spectroscopy image of pristine CNTs; (C) SEM image of pristine CNTs; (D) SEM image of dispersed CNTs in DW.

nanofluids could be expressed by:

$$\frac{k_{nf}}{k_{bf}} = \frac{3 + (\beta_{11} + \beta_{33})\varphi_p}{3 - \beta_{11}\varphi_p} \quad (1)$$

where k_{nf} and k_{bf} are the thermal conductivities of the nanofluid and the base fluid and φ_p is the volume fraction of the CNT.

$$\beta_{11} = \frac{2(k_{11}^c - k_{bf})}{k_{11}^c + k_{bf}}, \quad \beta_{33} = \frac{k_{33}^c}{k_{bf}} - 1 \quad (2)$$

The parameters k_{11}^c and k_{33}^c are the transverse and longitudinal equivalent thermal conductivities of the CNT, respectively.

$$k_{11}^c = \frac{k_p}{1 + \frac{2a_k k_p}{d_p k_{bf}}}, \quad k_{33}^c = \frac{k_p}{1 + \frac{2a_k k_p}{L_p k_{bf}}} \quad (3)$$

where d_p and L_p are, respectively, the diameter and length of the CNT, k_p is the CNT thermal conductivity, and a_k is the Kapitza radius expressed by $a_k = R_k k_{bf}$. R_k is the CNT–liquid interface thermal resistance, which is $8.33 \times 10^{-8} \text{ m}^2 \text{ K/W}$ [35]. The calculated results based on Nan's model are compared with the experimental data as shown in Fig. 2. A mean diameter of $\sim 25 \text{ nm}$ and a length of $\sim 50 \mu\text{m}$ (for an average aspect ratio of ~ 2000) CNTs dispersed in PAO was investigated by Choi et al. [12]. The calculated values predicted by Nan's model are much greater than the experimental data obtained

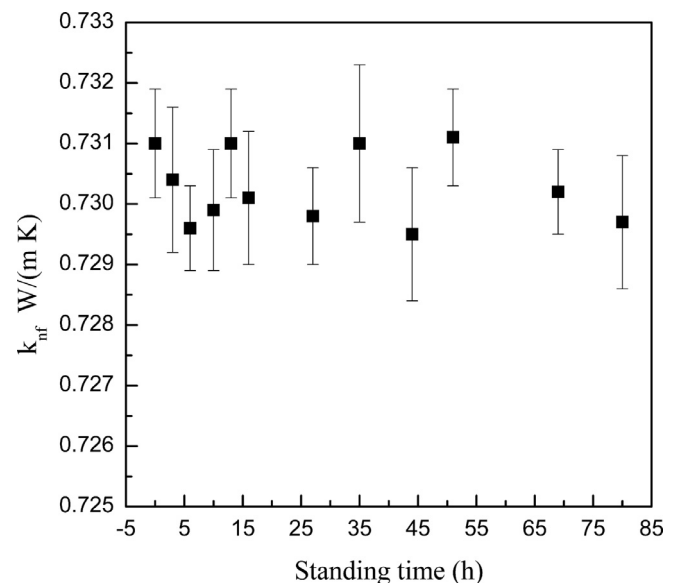


Fig. 5. Effective thermal conductivity of the 0.75 vol% nanofluid during the standing time at 80 °C.

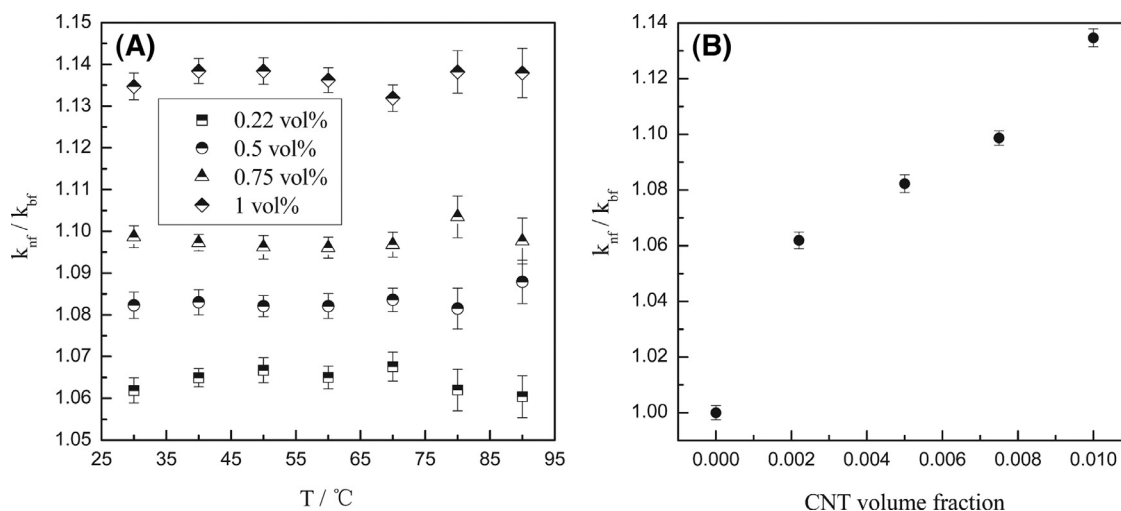


Fig. 6. Enhanced nanofluid thermal conductivity for: (A) various temperatures (30–90 °C) and CNT volume fractions (0.22–1 vol%); (B) different CNT volume fractions at 30 °C.

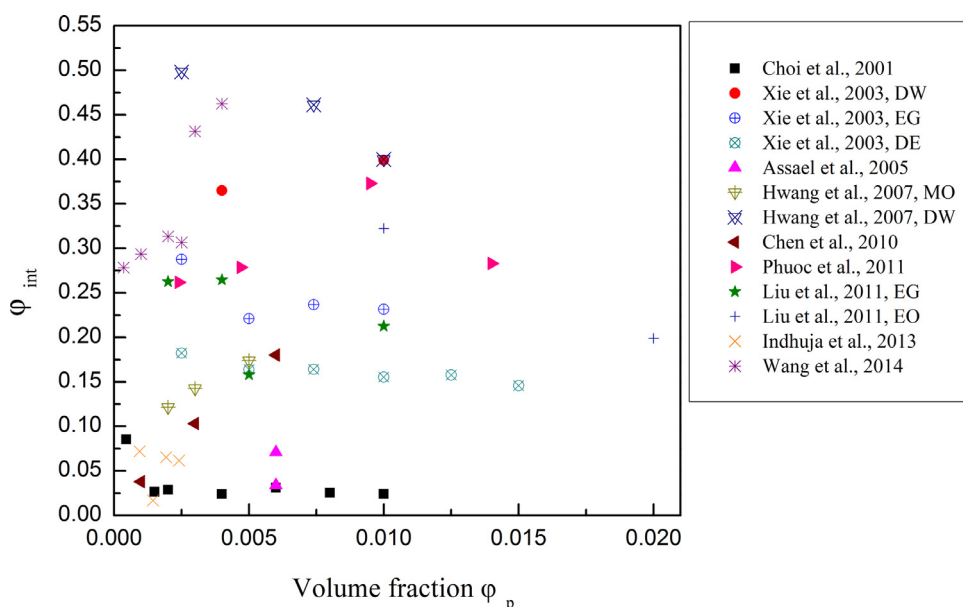


Fig. 7. Parameter φ_{int} calculated from our model with previous data [12–20].

by Choi et al. as the maximum thermal conductivity enhancement in Fig. 1.

The Nan's model overestimated the effective thermal conductivity of CNT-based nanofluids without considering the aggregation effects. When CNTs became agglomerated, the decreased SSA (specific surface area) of CNTs induced weak thermal transfer between CNTs, which reduced nanofluid thermal conductivity. Prasher et al. [24] proposed a model to describe the observed anomalous thermal conductivity enhancement reported in previous experiments. The data can be well explained by considering aggregation kinetics of spherical nanoparticles. This method is also applicable to CNT-based nanofluids taking aggregation into account.

$$\varphi_p = \varphi_{int}\varphi_a \quad (4)$$

where φ_{int} is the volume fraction of the CNTs in the aggregate and φ_a the volume fraction of the aggregates in the entire fluid (Fig. 3). The volume fraction of the aggregates φ_a decreases with increasing φ_{int} and $\varphi_p \leq \varphi_{int} \leq 1$. The thermal conductivity of the aggregates, k_{int} , is

expressed by rewriting the Nan's model.

$$\frac{k_{int}}{k_{bf}} = \frac{3 + (\beta_{11} + \beta_{33})\varphi_{int}}{3 - \beta_{11}\varphi_{int}} \quad (5)$$

where β_{11} and β_{33} are defined by Eq. (2). The effective thermal conductivity of CNT-based nanofluid is calculated by [36]

$$\frac{k_{nf}}{k_{bf}} = \frac{(k_{int} + 2k_{bf}) + 2\varphi_a(k_{int} - k_{bf})}{(k_{int} + 2k_{bf}) - \varphi_a(k_{int} - k_{bf})} \quad (6)$$

4. Results and discussions

4.1. Morphology and stability of nanofluids

Fig. 4(A) shows TEM photograph of the as received CNTs. The average outer diameter and length of these CNTs are about 11 nm and 10 μm , respectively. The I_D/I_G on the Raman spectrum is about 0.76 (Fig. 4(B)), indicating the CNTs were with high graphitization. Fig. 4(C) and (D) were the SEM images of the as received pristine CNTs and the

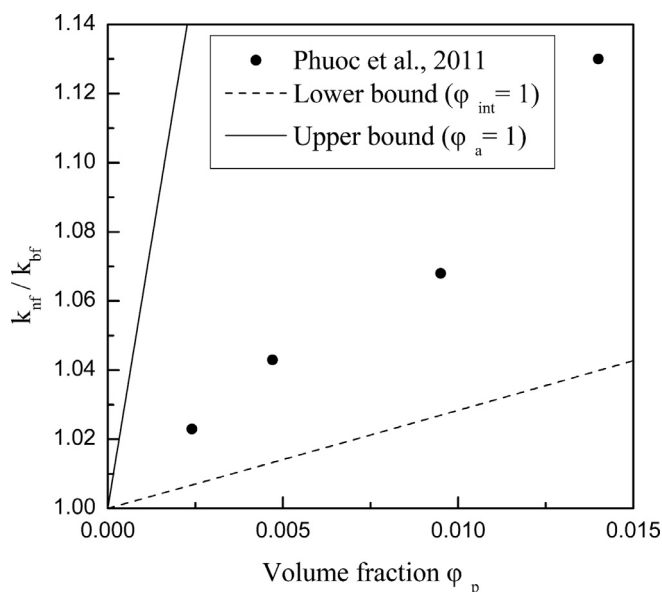


Fig. 8. Lower and upper bounds for CNT-based nanofluid thermal conductivity.

prepared CNTs in DW, respectively. The pristine CNTs were not only aggregated, but entangled with each other (Fig. 4(C)). The entanglements were broken in the as-prepared CNT-based nanofluids.

Fig. 5 exhibits the effect of the standing time (sedimentation time) on the effective thermal conductivity of nanofluid containing 0.75 vol% CNTs at 80 °C. The effective nanofluid thermal conductivities altered little within 80 h at 80 °C. There was no visible sedimentation of CNTs in the nanofluids, which demonstrated the good stability of the CNT-based nanofluids.

4.2. Effects of CNT concentration and temperature on effective thermal conductivity

The enhanced thermal conductivities of CNT/DW nanofluid were measured at different CNT volume fractions (0.22–1 vol%) and temperatures (30–90 °C), which is demonstrated in Fig. 6. The enhanced thermal conductivities were almost constant with increasing

temperature. The fluctuations of enhanced thermal conductivity became larger at higher temperature (>70 °C) (Fig. 6(A)). The effective thermal conductivity enhancement increased nonlinearly with increasing CNT volume fraction (Fig. 6(B)).

4.3. Comparison with models

Fig. 7 shows the various φ_{int} calculated from present model with previous data of the thermal conductivity enhancement of CNT-based nanofluids. The parameter φ_{int} is an empirical factor, which is influenced by CNT geometry, CNT volume fraction, type of fluid, the interaction between CNTs and base fluid, etc. It is impossible to deduce the accurate value of φ_{int} by theoretical model and φ_{int} needs to satisfy $\varphi_p \leq \varphi_{\text{int}} \leq 1$. The variant φ_{int} denotes CNT aggregation state in the base fluid. Higher φ_{int} means increased CNT concentration in the aggregate. The parameter φ_a is the volume fraction of the aggregates in the entire fluid which is defined by Eq. (4). When $\varphi_a = 1$ and $\varphi_p = \varphi_{\text{int}}$ (the nanofluid is a homogeneous suspension), $k_{\text{nf}} = k_{\text{int}}$, which means a medium composed wholly of CNT aggregates. When $\varphi_{\text{int}} = 1$ (the nanofluid is a well-dispersed suspension), there is only one CNT in each aggregate. The experimental data will lie between these two limits. The lower bound lies closer to thermal conductor in a series link (well-dispersed, separated), while the upper bound lies closer to a parallel conductor (chain-forming, clustered into percolation network). Chain-like aggregation of CNTs easily forms to conductive paths of high thermal conductivity, which can significantly enhance effective thermal conductivity [24,37]. Fig. 8 depicts the lower and upper bounds of present model compared with one experimental data [17]. The data lie between these two limits considering the CNT aggregate state in the base fluid. The bounds do not provide an accurate value of effective thermal conductivity but sets the restrictive limits taking the CNT aggregation into account.

The results predicted by the present model and Nan's model are compared with our experimental data (Fig. 9). The observed nonlinear results of the enhanced thermal conductivity with CNT concentrations (Fig. 6(B)) were predicted by the present model quite well, while the Nan's model predicts the enhanced thermal conductivities almost linearly with CNT loadings at small concentrations ($\varphi_p < 1$ vol%). Fig. 9(B) depicts the experimental data compared with present model at different temperatures. Because of high aspect ratio (~1000) used in our experiment, CNTs aggregated easily with each other.

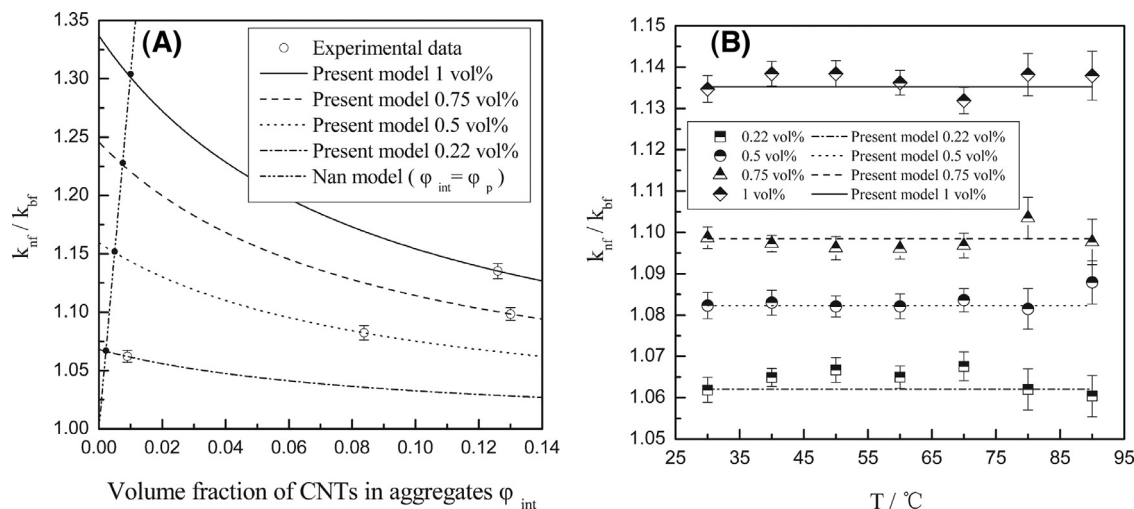


Fig. 9. Comparison of experimental data and present model: (A) various CNT volume fractions at 30 °C; (B) various temperatures and CNT volume fractions.

Consequently, contribution of other factors related to temperature such as Brownian motion induced nano-convection were negligible.

5. Conclusions

The stability of CNT/DW nanofluid was estimated by measuring effective thermal conductivity with various sedimentation times. The data of enhanced thermal conductivity of CNT-based nanofluid was collected at various CNT concentrations (0.22–1 vol%) and temperatures (30–90 °C). The thermal conductivity enhancement increased nonlinearly with higher CNT volume fractions. The temperature has a tiny role in the enhanced thermal conductivity of CNT-based nanofluids. A model of CNT-based nanofluid thermal conductivity based on the CNT aggregate state is proposed and the nanoparticle concentration in the aggregate φ_{int} is served as an empirical parameter. The present model gives the lower and upper limits of CNT-based nanofluid thermal conductivity. Chain-like aggregation of CNTs is beneficial to the thermal conduction which is conducive to develop nanofluids with higher thermal conductivity and performance to achieve ever-increasing cooling rates.

Acknowledgments

The authors acknowledge the support of the State Key Program of the National Natural Science Foundation of China (no. 51236004) and the Science Fund for Creative Research Groups (no. 51321002).

References

- [1] Choi SUS. Enhancing thermal conductivity of fluids with nanoparticles. In: Siginer DA, Wang HP, editors. Development and applications of non-Newtonian flows American society of mechanical engineers. New York, USA: Fluids Engineering Division (Publication) FED; 1995. p. 99–105.
- [2] Lee S, Choi SUS, Li S, Eastman JA. Measuring thermal conductivity of fluids containing oxide nanofluids. ASME J Heat Transfer 1999;121:280–9.
- [3] Eastman JA, Choi SUS, Li S, Yu W, Thompson LJ. Anomalously increased effective thermal conductivities of ethylene glycol-based nanofluids containing copper nanoparticles. Appl Phys Lett 2001;78:718–20.
- [4] Zhang X, Gu H, Fujii M. Effective thermal conductivity and thermal diffusivity of nanofluids containing spherical and cylindrical nanoparticles. J Appl Phys 2006;100 044325/1–044325/5.
- [5] Ghanbarpour M, Haghigi EB, Khodabandeh R. Thermal properties and rheological behavior of water based Al_2O_3 nanofluid as a heat transfer fluid. Exp Therm Fluid Sci 2014;53:227–35.
- [6] Jiang H, Li H, Zan C, Wang F, Yang Q, Shi L. Temperature dependence of the stability and thermal conductivity of an oil-based nanofluid. Thermochim Acta 2014;579:27–30.
- [7] Jiang H, Xu Q, Huang C, Shi L. Effect of temperature on the effective thermal conductivity of n-tetradecane based nanofluids containing copper nanoparticles. Particuology 2015 in press <http://dx.doi.org/10.1016/j.partic.2014.10.010>.
- [8] Iijima S. Helical microtubules of graphitic carbon. Nature 1991;354:56–8.
- [9] Berber S, Kwon YK, Tomanek D. Unusually high thermal conductivity of carbon nanotubes. Phys Rev Lett 2000;84:4613–16.
- [10] Che J, Cagin T, Goddard WA. Thermal conductivity of carbon nanotubes. Nanotechnology 2000;11:65–9.
- [11] Xie H, Cai A, Wang X. Thermal diffusivity and conductivity of multiwalled carbon nanotube arrays. Phys Lett A 2007;369:120–3.
- [12] Choi SUS, Zhang ZG, Yu W, Lockwood FE, Grulke EA. Anomalously thermal conductivity enhancement in nanotube suspension. Appl Phys Lett 2001;79:2252–4.
- [13] Xie H, Lee H, Youn W, Choi M. Nanofluids containing multiwalled carbon nanotubes and their enhanced thermal conductivities. J Appl Phys 2003;94:4967–71.
- [14] Assael MJ, Metaxa IN, Arvanitidis J, Christoflos D, Lioutas C. Thermal conductivity enhancement in aqueous suspensions of carbon multi-walled and double-walled nanotubes in the presence of two different dispersants. Int J Thermophys 2005;26:647–64.
- [15] Hwang Y, Lee JK, Lee CH, Jung YM, Cheong SI, Lee CG, et al. Stability and thermal conductivity characteristics of nanofluids. Thermochim Acta 2007;455:70–4.
- [16] Chen L, Xie H. Properties of carbon nanotube nanofluids stabilized by cationic Gemini surfactant. Thermochim Acta 2010;506:62–6.
- [17] Phuoc TX, Massoudi M, Chen RH. Viscosity and thermal conductivity of nanofluids containing multi-walled carbon nanotubes stabilized by chitosan. Int J Therm Sci 2011;50:12–18.
- [18] Liu MS, Lin MCC, Wang CC. Enhancements of thermal conductivities with Cu, CuO, and carbon nanotube nanofluids and application of MWNT/water nanofluid on a water chiller system. Nanoscale Res Lett 2011;6 297/1–297/13.
- [19] Indhuja A, Suganthi KS, Manikandan S, Rajan KS. Viscosity and thermal conductivity of dispersions of gum Arabic capped MWCNT in water: Influence of MWCNT concentration and temperature. J Taiwan Inst Chem Eng 2013;44:474–9.
- [20] Wang B, Hao J, Li Q, Li H. New insights into thermal conduction mechanisms of multi-walled carbon nanotube/ionic liquid suspensions. Int J Therm Sci 2014;83:89–95.
- [21] Koblinski P, Phillpot SR, Choi SUS, Eastman JA. Mechanisms of heat flow in suspensions of nano-sized particles (nanofluids). Int J Heat Mass Transfer 2002;45:855–63.
- [22] Jang SP, Choi SUS. Role of Brownian motion in the enhanced thermal conductivity of nanofluids. Appl Phys Lett 2004;84:4316–18.
- [23] Nan CW, Liu G, Lin Y, Li M. Interface effect on thermal conductivity of carbon nanotube composites. Appl Phys Lett 2004;85:3549–51.
- [24] Prasher R, Phelan PE, Bhattacharya P. Effect of aggregation kinetics on the thermal conductivity of nanoscale colloidal solutions (nanofluid). Nano Lett 2006;6:1529–34.
- [25] Jiang WT, Ding GL, Peng H. Measurement and model on thermal conductivities of carbon nanotube nanorefrigerants. Int J Therm Sci 2009;48:1108–15.
- [26] Wang JJ, Zhang RT, Gao JW, Chen G. Heat conduction mechanisms in nanofluids and suspensions. Nano Today 2012;7:124–36.
- [27] Jiang H, Li H, Xu Q, Shi L. Effective thermal conductivity of nanofluids considering interfacial nano-shells. Mater Chem Phys 2014;148:195–200.
- [28] Jiang H, Xu Q, Huang C, Shi L. The role of interfacial nanolayer in the enhanced thermal conductivity of carbon nanotube-based nanofluids. Appl Phys A 2015;118:197–205.
- [29] Sastry NNV, Bhunia A, Sundararajan T, Das SK. Predicting the effective thermal conductivity of carbon nanotube based nanofluids. Nanotechnology 2008;19 055704/1–055704/8.
- [30] Murshed SMS, Nieto de Castro CA. Superior thermal features of carbon nanotubes-based nanofluids – a review. Renew Sustain Energy Rev 2014;37:155–67.
- [31] Zhang Q, Huang JQ, Zhao MQ, Qian WZ, Wei F. Carbon nanotube mass production: Principles and processes. Chem Sus Chem 2011;4:864–89.
- [32] Zhang Q, Huang JQ, Qian WZ, Zhang YY, Wei F. The road for nanomaterials industry: A review of carbon nanotube production, post-treatment, and bulk applications for composite and energy storage. Small 2013;9:1237–65.
- [33] Assael MJ, Nieto de Castro CA, Roder HM. Experimental thermodynamics, vol. III: Measurement of the transport properties of fluids. Oxford: Blackwell Scientific Publications; 1991. p. 163–94.
- [34] Wu J, Zheng H, Qian X, Li X, Assael MJ. Thermal conductivity of liquid 1,2-dimethoxyethane from 243 K to 353 K at pressures up to 30 MPa. Int J Thermophys 2009;30:385–96.
- [35] Huxtable ST, Cahill DG, Shenogin S, Xue L, Ozisik R, Barone P, et al. Interfacial heat flow in carbon nanotube suspensions. Nat Mater 2003;2:731–4.
- [36] Nan CW, Birringer R, Clarke DR, Gleiter H. Effective thermal conductivity of particulate composites with interfacial thermal resistance. J Appl Phys 1997;81:6692–9.
- [37] Prasher R, Evans W, Meakin P, Fish J, Phelan P, Koblinski P. Effect of aggregation on thermal conduction in colloidal nanofluids. Appl Phys Lett 2006;89 143119/1–143119/3.